

Mach number M exceeds 1, the original LB model is not stable. The DVM is derived independent of Mach number. Therefore, we resort to the discretization on the left-hand side of Eq. (2) to make an accurate and stable LB scheme. Here we investigate a mixed scheme which is composed of a modified Lax-Wendroff [25] and an artificial viscosity.

As we know, the original Lax-Wendroff (LW) scheme is very dissipative and has a strong "smoothing effect". Obviously, it is not favorable when needing capture shocks in the system.

III. VON NEUMANN STABILITY ANALYSIS

We analyze the numerical stability of the FDLBM by means of von Neumann stability analysis [21,22]. In the analysis solution of finite-difference equation is written as the familiar Fourier series, and the numerical stability is evaluated by the magnitude of eigenvalues of an amplification matrix. The small perturbation $1/\epsilon$ is defined as: 公式 18-20

Several researchers have analyzed the stability of the incompressible LB models [21,26,27], it is found that there is not a single wave number being always the most unstable. For the 2D DVM by WT, G_{ij} is a matrix with 33×33 elements. Moreover, every element is related to the macroscopic variables (density, temperature, velocities), discrete velocities and other constants, so it is difficult to analyze with explicit expressions. We resort to use the software, Mathematica-5 to conduct a series of quantitative analysis. Now we show some numerical results of von Neumann analysis by Mathematica-5. The results will be shown by figures with curves for the maximum eigenvalue $|\omega|_{\max}$ versus $k\Delta x$.

Fig. 2 shows a comparison of the four different cases, (i) LB with only the central difference to the convection term, i.e. LB scheme based only on the first line of Eq. (17) (see the black line with squares); (ii) LB with Lax-Wendroff, i.e., LB scheme based on the first two lines of Eq. (17) (see the red line with circles); (iii) LB scheme based on lines 1 and 3 of Eq. (17) (see the green line with triangles); (iv) LB scheme based on the whole of Eq. (17) (see the blue line with triangles down). Moreover, it is worth noting that dissipation term in line 2 of Eq. (17) favors and dispersion term in line 3 disfavors the stability to some extent. Numerical experiments show that the dispersion term may effectively reduce the numerical oscillations near discontinuity and improves the accuracy (see Fig. 3 for an example). Fig. 4 shows the effects of various artificial viscosities to the stability. The other constants and macroscopic variables are unchanged. From this figure we can see some relevance: Strength of artificial viscosity has a large impact on the stability. LB works only within a certain range of artificial viscosity. In practical simulations, we generally take the smaller viscosity in favor of the accuracy.

Since the density ρ can be normalized to 1, we then need only investigate the effects of the other two physical quantities, temperature T and flow velocity u . Fig. 5 shows four cases with $T = 1$, $T = 5$, $T = 15$ and $T = 25$. Here $u_1 = 5$, $u_2 = 0$ and $\rho = 0$. When the other parameters are fixed, the numerical stability becomes better with the increasing of temperature. This can also be understood that higher temperature corresponds to higher sound speed and lower Mach number. Fig. 6 shows cases with varying flow velocities. The value of u_1 is altered from zero to 30 and $u_2 = 0$. Here $\rho = 0$, the other constants and macroscopic variables are unchanged. This figure clearly shows that the higher the Mach number, the larger the maximum eigenvalue, which answers why the numerical stability becomes worse with the increasing of Mach number of the fluid.

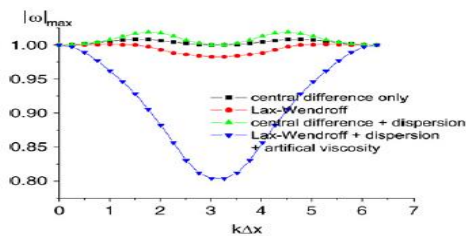


Fig. 2. (Color online) Stability analysis for four conditions.

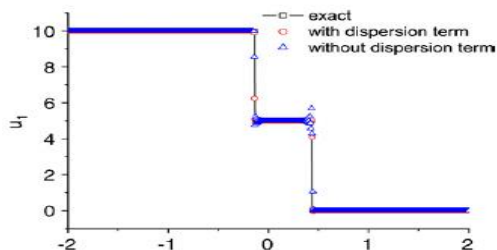


Fig. 3. (Color online) Effects of dispersion to simulation.

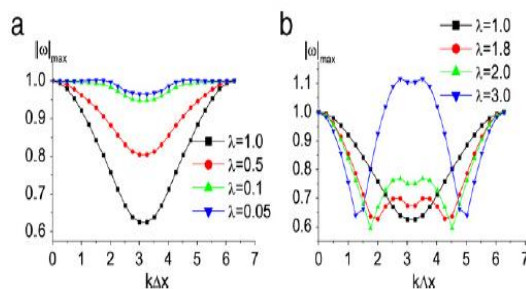


Fig. 4. (Color online) Effects of various artificial viscosities to the numerical stability.

IV. NUMERICAL TESTS AND ANALYSIS

In this section two kinds of typical benchmarks are used to validate the newly proposed scheme. The first kind is the Riemann problem [28]. The second one is the problem of shock reflection [29].

A. Riemann problems [28]

Here the two-dimensional model is used to solve the one-dimensional Riemann problem.

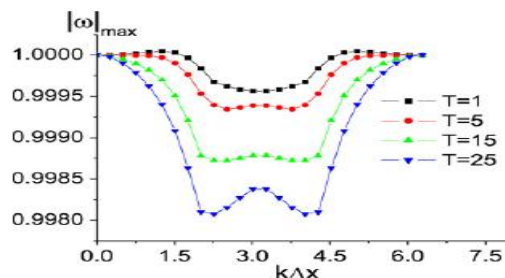


Fig. 5. (Color online) Influence of temperature T to numerical stability. $u_1 = 5$, $u_2 = 0$ and $\rho = 0$. The other physical quantities and model parameters are unchanged.

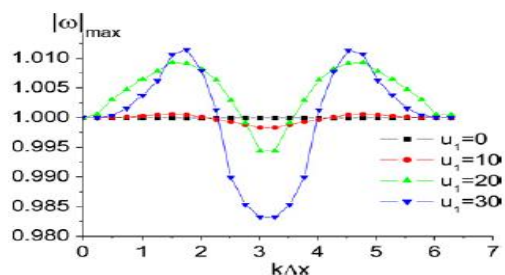


Fig. 6. (Color online) Influence of velocity u to numerical stability. Fig. 7 shows the computed density, pressure, velocity, temperature profiles at $t = 0.2$, where the circles are simulation results and solid lines with squares are analytical solutions.

Fig. 8 shows the results at $t = 0.2$, where the circles are simulation results and solid lines with squares correspond to exact solutions.

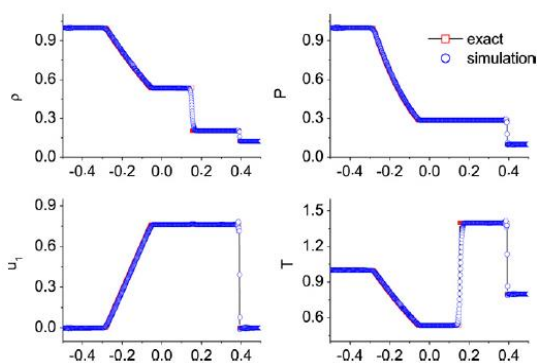


Fig. 7. (Color online) Comparison of numerical and theoretical results for the Sod shock tube, where $t = 0.2$. Solid lines with squares are for exact solutions and circles are for simulation results.

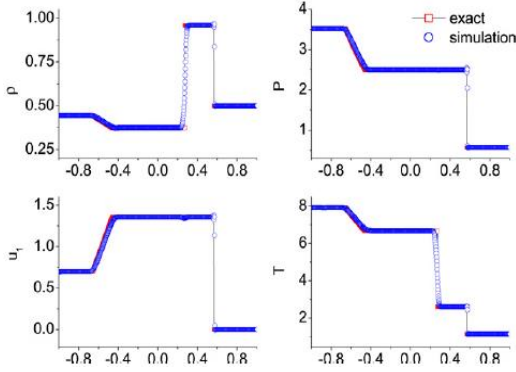


Fig. 8. (Color online) Comparison of numerical and theoretical results for the Lax shock tube at $t = 0.2$. Solid lines with squares are for exact solutions and circles are for simulation results.

The exact solution of this problem consists of two strong rarefaction waves and a weak constant contact discontinuity. Pressure near the contact discontinuity is very small, which brings certain difficulties to simulation. Temperature and density calculated by many schemes are negative. However, the improved model ensures the positivity of them. Successful simulation of this problem proves that the improved model is applicable to the low density, low-temperature flow simulations.

This is generally regarded as a difficult test. The exact solution contains a leftwards rarefaction wave, a contact discontinuity and a strong shock. It is generally used to check the robustness and accuracy. Fig. 10 gives comparison of the numerical and theoretical results at $t = 0.05$. Here $\gamma = 20$, other parameters are same as in the Sjogreen test. Successful simulation of this test proves that the improved model is applicable to flows with very high ratios of temperature and pressure.

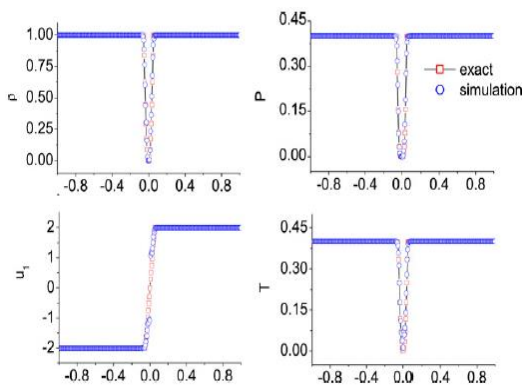


Fig. 9. (Color online) Comparison of numerical and theoretical results for the Sjogreen problem at $t = 0.018$. Solid lines with squares are for exact solutions, and circles are for simulation results.

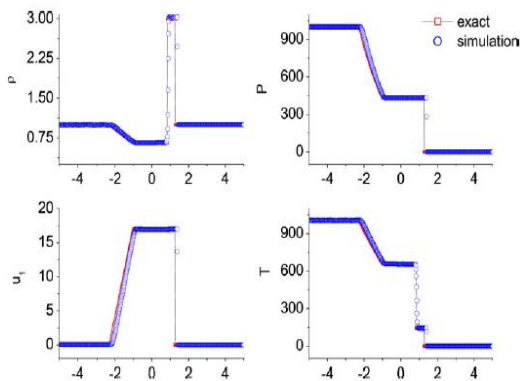


Fig. 10. (Color online) Comparison of numerical and theoretical results for the Colella explosion wave problem at $t = 0.05$. Solid lines with squares are for exact solutions and circles are for simulation results.

This is also a difficult test. Exact solution contains a leftwards shock, a right contact discontinuity and shock which spreading to right side.

Also, the left-shock spreads to right very slowly, which brings additional difficulties to the numerical method. Fig. 11 gives a comparison of the numerical and theoretical results at $t = 0.12$. The good agreement between the two sets of results shows again the robustness of the improved model.

We will present two gas dynamics simulations. Both are done on rectangular grid. The first is to recover a steady regular shock reflection. The second is the double Mach reflection of a shock off an oblique surface. This example is used in Ref. [30] as a benchmark test for comparing the performance of various difference methods on problem involving strong shocks.

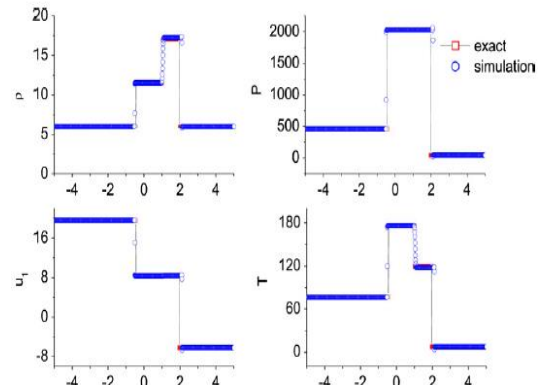


Fig. 11. (Color online) Comparison of numerical and theoretical results for collision of two strong shocks at $t = 0.12$. Solid lines with symbols are for exact solutions and symbols are for simulation results.

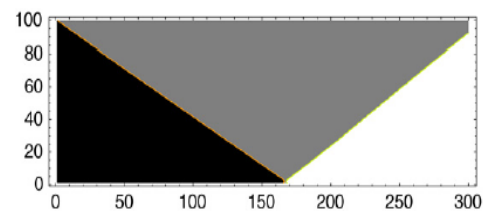


Fig. 12. (Color online) Density contour of steady regular shock reflection on a wall at $t = 0.2$. From black to white, the density increases.

B. Steady regular shock reflection

In the first test problem, the incoming shock wave with Mach number 20 has an angle of 30° to the wall. The computational domain is a rectangle with length 0.9 and height 0.3.

Fig. 12 shows contours of density at $t = 0.2$. The clear shock reflection on the wall agrees well with the exact solution.

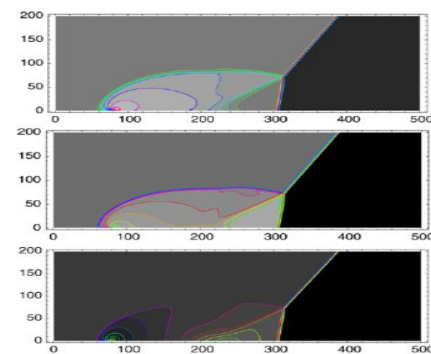


Fig. 13. (Color online) Contours of density (top), temperature (center), and u_1 (bottom) of the double Mach reflection problem

V. CONCLUSIONS AND DISCUSSIONS

A lattice Boltzmann model to the high-speed compressible Navier-Stokes system is presented. The new LB model is composed of the following components: the original DVM by Watari and Tsutahara, a modified Lax-Wendroff scheme and an additional artificial viscosity. Compared with the central difference scheme, the Lax-Wendroff contributes a dissipation term which is in favor of the

numerical stability, even though it is generally still not enough for high-speed flows. The introducing of the third-order dispersion term helps to eliminate some unphysical oscillations at discontinuity. The additional artificial viscosity compensates the insufficiency of the above-mentioned dissipation so that the LB simulation can continue smoothly. The adding of the dispersion and artificial viscosity terms should survive the dilemma of stability versus accuracy. In other words, they should be minimal but make the evolution satisfy the von Neumann stability condition. Due to the complexity, the analysis resorts to the software, Mathematica-5, and only some typical results are shown by figures.

Typical benchmark tests are used to validate the proposed scheme. Riemann problems, including the Sod, Lax, Sjogreen, Colella explosion wave, collision of two strong shocks, show good accuracy and numerical stability of the new scheme, even though they are generally difficult to resolve by the traditional computational fluid dynamics [28–31]. Regular and double Mach shock reflections are successfully recovered. These simulations show that the improved LB model may be used to investigate some long-standing problems, such as the transitions between regular and Mach reflections. By incorporating an appropriate equation of state, or equivalently, a free energy functional, or an external force, the present model may be used to simulate the liquid–vapor transition and the relevant flow behavior [1]. Future work includes a more complete description of the problem on numerical accuracy versus stability and the thermal lattice Boltzmann model for multi-phase flows.

ACKNOWLEDGMENTS

This work is supported by the National Natural Science Foundation of China (No. 11602066) and the National Science Foundation of Heilongjiang Province of China (QC2015058 and 42400621-1-15047), the Fundamental Research Funds for the Central Universities.

REFERENCES

- [1] S. Succi, "The Lattice Boltzmann Equation for Fluid Dynamics and Beyond," Oxford University Press, New York, 2001.
- [2] Q.F. Wu, W.F. Chen, "DSMC Method for Heat Chemical Nonequilibrium Flow of High Temperature Rarefied Gas, National Defence Science and Technology University Press," Beijing, 1999 (in Chinese).
- [3] Aiguo Xu, X.F. Pan, "Guangcai Zhang, Jianshi Zhu," J. Phys.: Condens. Matter 19 (2007) 326212; J. Phys. D: Appl. Phys. (in press); Commun. Theor. Phys. (in press).
- [4] F.J. Alexander, H. Chen, S. Chen, G.D. Doolen, Phys. Rev. A 46 (1992) 1967.
- [5] Gangwu Yan, Yaosong Chen, Shouxin Hu, Phys. Rev. E 59 (1999) 454.
- [6] H. Yu, K. Zhao, Phys. Rev. E 61 (2000) 3867.
- [7] C. Sun, Phys. Rev. E 58 (1998) 7283.
- [8] C. Sun, Phys. Rev. E 61 (2000) 2645.
- [9] C. Sun, A.T. Hsu, Phys. Rev. E 68 (2003) 016303.
- [10] T. Kataoka, M. Tsutahara, Phys. Rev. E 69 (2004) 035701(R); Phys. Rev. E 69 (2004) 056702.
- [11] M. Watari, M. Tsutahara, Phys. Rev. E 67 (2003) 036306; Phys. Rev. E 70 (2004) 016703.
- [12] Aiguo Xu, Europhys. Lett. 69 (2005) 214; Phys. Rev. E 71 (2005) 066706; Prog. Theor. Phys. (Suppl.) 162 (2006) 197.
- [13] R. Benzi, S. Succi, M. Vergassola, Phys. Rep. 222 (1992) 145; D.A. Wolf-Gladrow, "Lattice Gas Cellular Automata and Lattice Boltzmann Models," Springer-Verlag, New York, 2000; H. Chen, S. Kandasamy, S. Orszag, R. Shock, S. Succi, V. Yakhot, Science 301 (2003) 633.
- [14] W.A. Yong, L.S. Luo, Phys. Rev. E. 67 (2003) 1063.
- [15] A. Xiong, Acta Mech. Sinica (English Series) 18 (2002) 603.
- [16] F. Tosi, S. Ubertini, S. Succi, H. Chen, I.V. Karlin, Math. Comput. Simul. 72 (2006) 227.
- [17] S. Ansumali, I.V. Karlin, J. Stat. Phys. 107 (2002) 291; S. Ansumali, I.V. Karlin, H.C. Ottinger, Europhys. Lett. 63 (2003) 798.
- [18] Y. Li, R. Shock, R. Zhang, H. Chen, J. Fluid Mech. 519 (2004) 273.
- [19] V. Sofonea, A. Lamura, G. Gonnella, A. Cristea, Phys. Rev. E 70 (2004) 046702.
- [20] R.A. Brownlee, A.N. Gorban, J. Levesley, Phys. Rev. E 75 (2007) 036711.
- [21] T. Seta, R. Takahashi, J. Stat. Phys. 107 (2002) 557.
- [22] X.F. Pan, Aiguo Xu, "Guangcai Zhang, Song Jiang," Int. J. Mod. Phys. C (in press); Preprint Version: arXiv:0706.0405v1.
- [23] Aiguo Xu, G. Gonnella, A. Lamura, Phys. Rev. E 74 (2006) 011505; Phys. Rev. E 67 (2003) 056105; Physica A 331 (2004) 10; Physica A 344 (2004) 750; Physica A 362 (2006) 42; Aiguo Xu, Commun. Theor. Phys. 39 (2003) 729.
- [24] P. Bhatnagar, E.P. Gross, M.K. Krook, Phys. Rev. 94 (1954) 511.
- [25] R. Liu, Q. Shu, "Some New Methods in Computational Fluid Dynamics," Science Press, Beijing, 2003 (in Chinese).
- [26] J.D. Sterling, S. Chen, J. Comput. Phys. 123 (1996) 196.
- [27] X.D. Niu, C. Shu, Y.T. Chew, T.G. Wang, J. Stat. Phys. 117 (2004) 665.
- [28] G. Lv, "Advances in the Study of the Finite-Point Methods," Research Report of China Academy of Engineering Physics, Beijing, 2006 (in Chinese).
- [29] H. Zhang, "Research on High Order Accurate Numerical Methods for Fluid Dynamics (in Chinese)," Ph.D. theses of Nanjing University of Aeronautics and Astronautics, Nanjing, 2005.
- [30] P.R. Woodward, P. Colella, J. Comput. Phys. 54 (1984) 115.
- [31] Xijun Yu, Qingfang Dai, Numer. "Methods Partial Differential Equations," 22 (2006) 1455; Qingfang Dai, Xijun Yu, SIAM J. Sci. Comput. 28 (2006) 805.